TELKOMNIKA, Vol. 11, No. 10, October 2013, pp. 5725 ~ 5733
ISSN: 2302-4046

Analysis on the Key Parameters of Aerospace Microminiaturization Decelerator

Xiangyang Jin*, Jianyuan Feng, Lili Zhao
School of Light Industry, Harbin University of Commerce, Harbin 150028, Heilongjiang, China
*Corresponding author, e-mail: jinxiangyang@126.com

Abstract

A high efficiency special transmission decelerator is designed by scheme design, structural design, optimization design, and return difference analysis and computer simulation. Small teeth difference transmission with the first level bevel gear pair and the second level beveloid gear pair is adopted as the form of transmission in the decelerating system. Great torque and big bending moment are available by transmission ratio formula deduction, force analysis and strength analysis. The particle swarm optimization and the genetic algorithm have been combined and the mutation operator optimization model has been proposed to optimize the design of decelerator. Then the transmission with large transmission ratio, high torque, high power and high precision will be realized in small space. This model has solved the problems of particle swarm optimization in mechanical design. For example, there are more variables, it is constrained and it is easily precocious. This model has provided the theoretical basis for the optimum design of microminiaturization gear system.

Keywords*: Return Difference Analysis, Particle Swarm, Mutation Operator*

1. Introduction

Microminiaturization decelerator for aerospace purpose adopts the first level bevel gear transmission and the second level small teeth difference inner gearing beveloid gear transmission to successfully apply beveloid gears to decelerators. It replaces the cycloidal pin wheel in RV transmission, which helps the decelerator to not only inherit RV decelerator's advantages of small volume, great transmission ratio, great carrying capabilities, large rigidity, high kinematic accuracy and high transmission efficiency etc. But also make use of the structural features of the beveloid gear to conveniently adjust the gearing backlash, reduce the return difference for purpose of precision transmission [1, 2]. The structural diagram is shown in Figure 1, the first level adopting bevel gear transmission and the second level consisting of a parallelogram linkage and gear mechanisms. Excentric layout is adopted for the output shaft and supporting axle serving as the crank of the parallelogram linkage; the internal gear and output shaft are fixedly connected or made as a whole [3, 4]. During the operation, the external gear is driven by the input shaft and supporting axle to do translational motion. Then the motive power is output through the output shaft by gearing of internal and external gears.

The size of decelerator should not be much larger due to the limitation. Therefore, it is critical to employ a good optimization algorithm to optimize the parameters of decelerator for this microminiaturization transmission device. As the modification coefficients of the thickened gear are different in different sections, if the modification coefficients are designed to present the linear changes along the axis, the tooth crest will have a certain taper along the axial direction [5, 6]. Afterwards, the gear meshing backlash can be adjusted through controlling the axial displacement so as to achieve the purpose of adjusting the backlash or eliminating the backlash. At the same time, this transmission has the small gear backlash, the high rigidity, the large carrying capacity and the smooth operation, which is suitable for the mechanical drive that has high precision, high rotation speed and that can be accelerated and decelerated in short time. This is the driving body that is greatly needed by the aerospace microminiaturization decelerator and other precise machines.

Based on this demand, the thickened gear has been firstly applied in the microminiaturization decelerator, which not only inherits the various merits without the teeth difference driving, but also adjusts the meshing backlash and reduces the gear backlash as well

Received February 17, 2013; Revised July 1, 2013; Accepted July 15, 2013

as achieves the precision driving. According to the characteristics of mechanical optimum design, it has been improved based on the particle swarm optimization. The particle swarm optimization and the genetic algorithm have been also successfully applied in the optimum design of the parameters of microminiaturization decelerator [7]. The practice has shown that

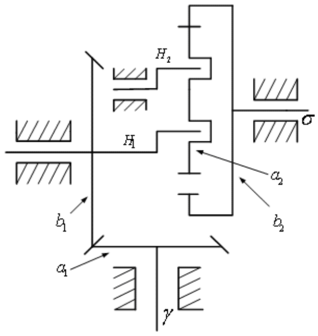

Figure 1. Driving diagram of microminiaturization decelerator

the improved particle swarm optimization in this paper is effective in the optimum design of decelerators.The crank shaft with power input in the mechanism is called input shaft and the crank shaft without power input is called supporting axle. In this kind of transmission, the external gear makes translational motion instead of planetary motion as in transmission of general planetary gear and the internal gear makes fixed-axis rotation.The structure of microminiaturization decelerator is consist of the first level bevel drive transmission and second level small teeth internal gearing beveloid gear transmission [8]. In the transmission scheme, it is set that the scheme code is represented by a letter with two subscripts. The first subscript represents basic driving members and the second subscript represents basic driven members. The first part of the transmission code is the high speed gear transmission basic components. The corner mark is represented with 1; the basic components for low speed gear transmission are represented by 2. For the convenience of the follow up theoretical calculation, input shaft is represented by γ, output shaft by σ and the excentric shaft by H_1 and H_2.

2. Deduction in Transmission Ratio

The transmission ratios of the first level bevel gear pair and the second level beveloid gear are as follows:

$$i_1 = z_{b1} / z_{a1}$$
$$i_2 = z_{a2} / (z_{b2} - z_{a2}) \quad (1)$$

The total transmission ratio $i_{\tau\sigma} = i_1 \cdot i_2$.

Torque acting on the bevel pinion $T_{a1} = T_\sigma / i_{\tau\sigma}$.

3. Force Analysis and Calculation

With the advancement in networking and multimedia technologies enables the distribution. Although encryption can provide multimedia content once a piece of digital content is decrypted, the dishonest customer can redistribute it arbitrarilys.

Tangential force acting on the reference circle

$$F_{ta1} = 2000 T_{a1} / d_{ma1} \quad (2)$$

In the formula, d_{ma1} ——Diameter of the reference circle on the bevel pinion (mm).

Torque acting on the bevel gear wheel $T_{b1} = T_{\sigma} / i_2$.

Tangential force acting on the reference circle

$$F_{tb1} = 2000 T_{b1} / d_{mb1} \tag{3}$$

In the formula, d_{mb1} ——Diameter of the reference circle on the bevel gear wheel (mm).

Force on the tooth of the gear with small difference [9, 10]

$$F_{t2} = 1.2 T_{\sigma} z_{a2} / (d_{a2} z_{b2}) \tag{4}$$

The bearing of internal beveloid toothing excentric shaft with small difference is installed between the external gear and the excentric shaft. The layout of the output mechanism shall also be considered for the external gear. Therefore the dimension of the excentric shaft is restricted to a certain degree. As experience proves, the service life of the bearing of the excentric shaft is the key factor to influence the carrying capability of this kind of transmission.

The force diagram of the external gear is shown in Figure 2. The normal force acting on the external fear by the internal gear is F. As it is double eccentric, theoretically, $F = T_{\sigma} / (2 r_{a2})$.

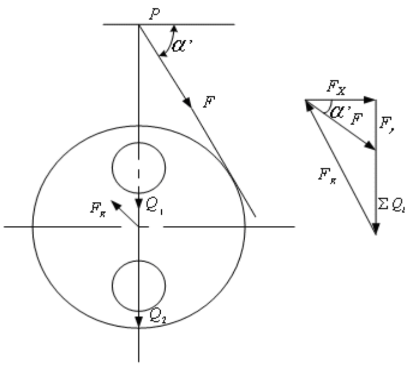

Figure 2. Forced estate of external gear

Considering the uneven force, it shall be calculated by the following formula

$$F = 0.6 T_{\sigma} / r_{a2} \tag{5}$$

In the formula, r_{a2} ——Radius of the reference circle on the external beveloid gear.

F can be resolved into F_x and F_y .

$$F_x = 0.6 T_{\sigma} \cos\alpha' / r_{\alpha 2}$$
$$F_y = F_x \tan\alpha' \tag{6}$$

The maximum resultant force acting on external gear from various excentric shafts is as below [9]:

$$(\sum Q_i)_{\max} = 2.4 T_{\sigma} / (R_W Z_W \sin\frac{\pi}{Z_W}) \tag{7}$$

In the formula, R_W ——Radius of pin hole distribution circle (mm);

Z_W ——Number of the pin holes.

By force polygon, the force acting on the external gear R_1 is as below:

$$F_R = \sqrt{F_x^2 + \left[(\sum Q)_{\max} + F_y \right]^2} \tag{8}$$

4. Analysis on Strength of Shaft and Calculation

Safety coefficient checking calculation for shaft includes the following two aspects: Fatigue strength safety coefficient check and the static strength safety coefficient check. The fatigue strength safety coefficient is checked after preliminary calculation and structural design, in accordance with the factors such as actual dimension, bending moment borne, turning moment diagram and considering factors such as stress concentration, surface state, size influence and the fatigue limit of the shaft materials for calculating the fatigue safety coefficient of dangerous sections on the shaft to see whether the requirements are met or not. Checking the safety coefficient of the static strength is to calculate the safety coefficient of the static strength on the dangerous sections of the shaft in accordance with yield strength of the shaft materials and the maximum transient load acting on the shaft.

The formula for checking and calculating the fatigue strength safety coefficient of the shaft is as below:

$$S = S_\sigma S_\tau / \sqrt{S_\sigma^2 + S_\tau^2} \geq [S] \tag{9}$$

In the formula, S_σ ——safety coefficient under action of bending moment is considered;
S_τ ——only the safety coefficient under the action of torque is considered;
$[S_2]$ ——allowable safety coefficient calculated in accordance with fatigue strength.

$$S_\sigma = \sigma_{-1} / (\frac{K_\sigma}{\beta \varepsilon_\sigma} \sigma_\alpha + \psi_\sigma \sigma_m)$$
$$S_\tau = \tau_{-1} / (\frac{K_\tau}{\beta \varepsilon_\tau} \tau_\alpha + \psi_\tau \tau_m) \tag{10}$$

The formula for checking and calculating the static strength safety coefficient of the shaft is as below

$$S_s = \frac{S_{s\sigma} S_{s\tau}}{\sqrt{S_{s\sigma}^2 + S_{s\tau}^2}} \geq [S_s] \tag{11}$$

In the formula, S_σ ——only the safety coefficient when bent is considered;
S_τ ——only the safety coefficient when twisted is considered;
$[S]$ ——allowable safety coefficient calculated in accordance with static yield strength.

$$S_{s\sigma} = W \sigma_s / M_{\max} \qquad S_{s\tau} = W_p \tau_s / T_{\max} \tag{12}$$

5. Improvement of Particle Swarm Optimization

The particle swarm optimization (PSO) starts from a set of random solutions and searches for the optimal solutions through the iteration.The corresponding particle is called the individual particle $p_{p,d}$. The particles will update their own speed and positions according to the following two formulas [11].

$$V = \omega * V + c_1 * rand * (pBest - \Pr esent) + c_2 * rand * (gBest - \Pr esent) \quad (13)$$

$$\Pr esent = \Pr esent + V \quad (14)$$

In this formula, V —— the speed of particle;
$\Pr esent$ —— the current position of particle;
$rand$ —— the random number between [0, 1];
c_1, c_2 —— the learning factor, generally speaking;
ω —— the weighted factor, the value of which is usually from 0.1 to 0.9.

According to formula (13) and (14), the position of particle in next time is determined by the current position and the current speed. The speed determines the distance and the direction of speed determines the heading direction of particles. According to formula (13), the current speed of particles is determined by three factors: the original speed, the individual extreme $pBest$ and the global extreme $gBest$. The global extreme $gBest$ is the optimal solution at present. If the algorithm appears the premature convergence, the global extreme $gBest$ must be the local optimal solution. Combined with formula (13), if the global extreme is changed (the mutation operation will be introduced to the genetic algorithm), the heading direction of particles will be changed. Then the particles will enter other areas for search. In the subsequent search process, the algorithm may find the new individual extreme $pBest$ and the global extreme $gBest$. Through the cycling, the algorithm will find the global optimal solution. This is the basic idea to improve the particle swarm optimization methods proposed in this paper.

Considering that the particle may find a better position under the influence of current $gBest$, so the mutation operation will be designed as a random operator by the new algorithm, namely, $gBest$ which meets the mutation conditions will be mutated according to the certain probability ρ. The calculation formula of ρ can be shown as:

$$\rho = \begin{cases} k, \sigma^2 < \sigma_d^2 and F(gBest) > F_d \\ 0, others \end{cases} \quad (15)$$

In this formula, k selects the any value between [0.1, 0.3]. The value of σ_d^2 is related to the actual problems, which is usually less than the maximum of σ^2. F_d can be set as the theoretical optimal value. The minimum situation is considered here. σ^2 is the group fitness variance of particle swarms, the calculation formula of which can be shown as:

$$\sigma^2 = \sum_{i=1}^{n} \left(\frac{F_i - F_{avg}}{F}\right)^2 \quad (16)$$

In this formula, n —— the number of particles in particle swarms;
F_i —— the fitness of the i particle;
F_{avg} —— the current average fitness of particle swarms.

The specific steps of the mutation operation of $gBest$ are: assuming that we have obtained a set of local optimal point X_1 through employing the particle swarm optimization. X_1 should be translated into the binary code (i.e. 0, 1 string). $X_1 = (x_1, x_2, ..., x_D)$, in which x_i ($i = 1, 2, ..., D$) is the i position in the binary expression. Afterwards, the mutation operation in genetic algorithm has been employed to change X_1 into X_2, namely a probability is adopted to randomly change the bits in X_1 binary expression [12]. Then the corresponding coding will be also changed (from 0 to 1 or from 1 to 0) so as to obtain a group of new solutions. After comparing the fitness values of X_1 and X_2, it is required to eliminate the solutions which are poorer than X_1 and save the solutions which are more excellent than X_1. After finishing the set number of genetic mutation, we will get the solution X_2 which is more optimal than X_1. Then it is necessary to adopt the particle swarm algorithm to conduct the optimization in the neighborhood.

6. Applications

6.1. The Determination of Design Variables

According to the design requirements, the variables can be shown in Table 1 and there are a total of eight variables.

Table 1. Parameters of Microminiaturization Decelerator (mm)

Level	Modulus	Teeth number of small gear	Teeth number of large gear	Teeth width
First level	m_1	Z_{a1}	Z_{b1}	b_1
Second level	m_2	Z_{a2}	Z_{b2}	b_2

6.2. The Determination of Design Constraints

According to the requirements of transmission ratio of decelerator

$$h_1(x) = 120 - \frac{z_{b1}}{z_{a1}} \cdot \frac{z_{a2}}{z_{b2} - z_{a2}} = 0 \tag{17}$$

Due to the limitations of the size of decelerator, the size of motor should be less than 82mm×120mm×60mm.

$$\begin{aligned} g_1(x) &= 82 - b_1 \sin\delta_{b1} - m_2 z_{b2} \geq 0 \\ g_2(x) &= 60 - b_1 \cos\delta_{b1} - b_2 \geq 0 \end{aligned} \tag{18}$$

In this formula, δ_{b1} —— the reference cone angle of large bevel gear.

The contact fatigue strength of bevel gear

$$g_3(x) = \sqrt{\frac{K_A K_V K_{H\beta} K_{H\alpha} F_t}{m_1 z_{a1} b_1} \cdot \frac{\sqrt{u^2+1}}{u}} \cdot Z_{M-B} Z_H Z_E Z_{LS} Z_\beta Z_K \leq \sigma_{HP} \tag{19}$$

In this formula, F_t —— the tangential force of meshing gear;

u —— the transmission ratio of meshing gear.

The bending strength of the root of bevel gear

$$g_4(x) = \frac{K_A K_V K_{F\beta} K_{F\alpha} F_t}{b_1 m_1} Y_{FS} Y_E Y_K Y_{JS} \leq \sigma_{FP} \tag{20}$$

The bending strength of the root of thickened gear

$$g_5(x) = \frac{F_t}{b_2 m_2} K_A K_V K_{F\beta} K_{F\alpha} Y_{FS} Y_{\varepsilon\beta} \leq \sigma_{FP} \tag{21}$$

Constraints of coincidence degree of bevel gear pair transmission in the first level

$$g_6(x) = 1.2 - \varepsilon_1 > 0 \tag{22}$$

In this formula, ε_1 —— the coincidence degree of bevel gear pair in the first level.

The constraints of the coincidence degree of thickened gear pair in the second level

$$g_7(x) = 1.1 - \frac{1}{2\pi}((z_{b2} - z_{a2})\tan\alpha' + z_{a2}\tan\alpha_{aa2} - z_{b2}\tan\alpha_{ab0} - b_2\sin\beta/(\pi m_2) > 0 \quad (23)$$

In this formula, β —— the helix angle of thickened gear (°);

α' —— the engaging angle of thickened gear pair (°);

$\alpha_{aa2}, \alpha_{ab0}$ ——the pressure angle of the addendum in the cross section in big end of thickened external gear and the pressure angle of the addendum in the small section of thickened internal gear.

In this formula, the corner mark a represents the thickened external gear and b represents the thickened internal gear. 2 represent the cross section in big end of thickened gear and 0 represents the cross section in small end. The value can be calculated according to the following formulas:

$$\alpha_{a2} = \arccos\frac{m_2 z_{a2}\cos\alpha}{r_{aa2}}$$

$$\alpha_{ab0} = \arccos\frac{m_2 z_{b2}\cos\alpha}{r_{ab0}} \quad (24)$$

The overlap and interference constraints of tooth profile of internal meshing thickened gear.The internal meshing thickened gear pair in decelerator is the one-tooth transmission and the tooth profiles are easily overlapped and interfered. As the modification coefficients of each cross section of thickened gear present the linear changes along the axial direction, when the overlap and interference constraints of tooth profile are established, other cross sections will certainly meet the requirements as long as the tooth profiles in the cross sections of big end and small end are not overlapped. The conditions that constrain the cross sections in big end and small end of internal thickened gear pair to be overlapped and interfered are respectively:

$$g_8(x) = z_{a2}(\delta_{a0} + inv\alpha_{aa0}) - z_{b2}(\delta_{b0} + inv\alpha_{ab0}) + (z_{b2} - z_{a2})inv\alpha' > 0 \quad (25)$$

In this formula, $\delta_{a0} = \arccos(\frac{d_{ab0}^2 - d_{aa0}^2 - 4a^2}{4ad_{aa0}})$ $\delta_{b0} = \arccos(\frac{d_{ab0}^2 - d_{aa0}^2 + 4a^2}{4ad_{ab0}})$

a —— the center distance of thickened gear pair, which can be calculated by following formula

$$a = \frac{m_2(z_{b2} - z_{a2})}{2\cos\alpha'}\cos\alpha \quad (26)$$

$$g_9(x) = z_{a2}(\delta_{a2} + inv\alpha_{aa2}) - z_{b2}(\delta_{b2} + inv\alpha_{ab2}) + (z_{b2} - z_{a2})inv\alpha' > 0 \quad (27)$$

In this formula, δ_{a2} and δ_{b2} can take calculation formula of δ_{a0} and δ_{b0} as reference.

The Matlab language programming has been employed and the running results in computers can be shown in Table 2.

Table 2. Results of Optimization in Microminiaturization Decelerator (mm)

Level	Modulus	Teeth number of small gear	Teeth number of large gear	Teeth width
First level	m_1=1	Z_{a1}=18	Z_{b1}=62	b_1=9
Second level	m_2=1.5	Z_{a2}=35	Z_{b2}=36	b_2=12

7. Finite Element Analysis on Beveloid Gear

During the gear's meshing process, the stress distribution varies along the contact points. Classical gear design theory approximates the distributed load as concentrated force applied to the reference circle, with some errors in the calculation. Calculation by finite element method can effectively simulate the real meshing process of the gear and observe the changing conditions of various stresses. Classical gear analysis method supposes the gear to be a rigid body, without considering the influence of the gear deformation on the contact force on gear surface and the overlap ratio of the gear pair [13]. Finite element, however, treats the gear as a flexible piece. In this thesis, LS-DYNA finite element analysis software is adopted for finite element simulation analysis on the meshing process of the gear, with the aim of analyzing distribution of its bending stress and contact stress. The maximum contact stress of the gear shall be, at any time, on the meshing position of the gear tooth and the corresponding stress concentration is produced on the root of the gear tooth. The distribution of transient contact stress at the root of a single tooth is shown in Figure 3.Judging by the equivalent stress in Figure 3, a conclusion can be made that the contact stress on tooth surface is of linear distribution and the stress on both sides is a little greater. In general, the stress distribution is even. The analyzed stress result shows that the gear designed in this thesis meets the requirements for contact strength. Besides, it can also be observed that the overlap ratio of the gear pair is greater than 1.2 through the meshing situation of two adjacent teeth. The distribution of transient contact stress at the root of a single tooth is shown in Figure 4.

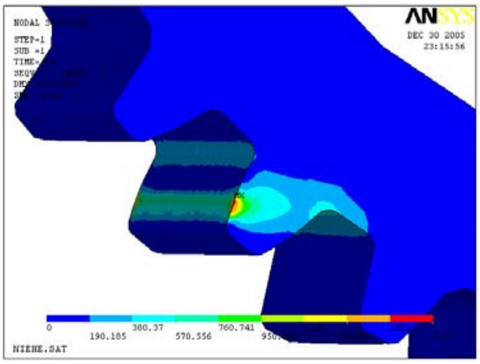

Figure 3. Contact stress of external beveloid gear

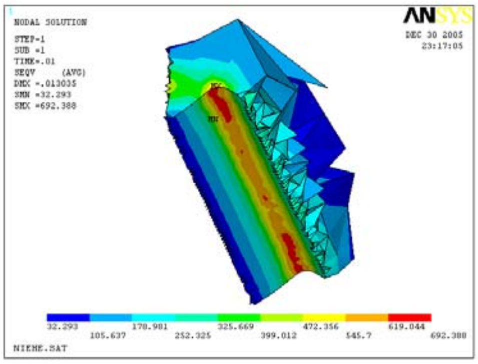

Figure 4. Contact stress of tooth root in external beveloid gear

8. Conclusion

After analyzing and researching the decelerators, transmission ratio deduction, force calculation and strength analysis for decelerators are done to lay the foundation for the structural design and provide theoretical basis for virtual prototype model establishing and computer simulation.

The particle swarm optimization and the genetic algorithm have been combined and the mutation operator optimization model has been proposed. This model has solved the problems of particle swarm optimization in mechanical design. For example, there are more variables, it is constrained and it is easily precocious. The improved particle swarm optimization has been also successfully applied in the optimum design of microminiaturization decelerator.

According to the optimization results, the transmission ratio of deceleration system, the torque and force suffered by the components, the transmission ratio of whole system have been obtained, which has provided the basis for the virtual prototype modeling of decelerator.

Acknowledgements

This work was supported by Scientific Research Fund of Heilongjiang Provincial Education Department (No. 1252CGZH18), Twelfth Five-year Plan Issues for Heilongjiang High

Education Scientific Research (No. HGJXHB2110792), and the Youth Science and Technology Innovative Talents Project of Harbin Science and Technology Bureau (No. 2012RFQXG076).

References

[1] K Kondo. Study on Tooth Profiles of the Harmonic Driver. *Transactions of ASME*. 2003; 112(2): 131-137.
[2] Sunage T. Differential reducers using internal gears with small tooth number difference. *Bulletin of JSME*. 2005; 108(5): 28-39.
[3] Xiangyang Jin, Xiangyi Guan, Lili Zhao. Spectral analysis and independent component separation for aero-engine rotor vibration. *International Review on Computers and Software*. 2012; 7(5): 2740-2744.
[4] Yoon KY, Rao SS. Dynamic Load Analysis of Spur Gears Using a New Tooth Profile. *Journal of Mechanical Design*. 1996; 118(1): 1-6.
[5] Moschioni G, Saggin B, Tarabini M. Prediction of data variability in hand-arm vibration measurements. *Measurement: Journal of the International Measurement Confederation*. 2011; 44(9): 1679-1690.
[6] Zhang Y, Litvin FL, Hnadschuh KF. Computerized Design of Low-Noise Face-Milled Spiral Bevel Gears. *Mechanism and Machine Theory*. 1995; 30(8): 1171-1178.
[7] Srinil, Narakorn. Analysis and prediction of vortex-induced vibrations of variable-tension vertical risers in linearly sheared currents. *Applied Ocean Research*. 2011; 33(1): 41-53.
[8] Reinald Schumann.Vom Spielarmen Zum Spielfreien Getriebe-Firmenportrait der Alpha Getriebebau Gmbh. *Antriebstechnik*. 1990; 29(2): 10–15.
[9] Humbert. Spielfreie Planetengetrieke Funktion und Anwendung. *AGT Dok*. 1991; 20(3): 90-91.
[10] Red School, Andreas Rouhut, Frank Funk. Schneckengetrieke Mit Spieleinstellbarer Verzahnung. *Antriebstechnik*. 1991; 30(4):94–97.
[11] Bossi L, Rottenbacher C, Mimmi, G Magni L. Multivariable predictive control for vibrating structures: An application. *Control Engineering Practice*. 2011; 19(10): 1087-1098.
[12] K Umezawa, T Suzuki, H Houjoh. Estimatin of Vibration of Power Transmission Helical Gears by Means of Performance Diagrams on Vibration. *JSME International Journal*. 1988; 31(4): 598-605.
[13] Kamali M, Ataei M. Prediction of blast induced vibrations in the structures of Karoun III power plant and dam. *JVC/Journal of Vibration and Control*. 2011; 17(4): 541-548.